Computer Assisted Mechanics and Engineering Sciences, 10: 629–640, 2003.

Folded-plate structures with openings – analysis and optimization

Bogdan Szybiński, Andrzej P. Zieliński
Institute of Mechanics & Machine Design, Cracow University of Technology, Poland

Marek Karaś*
Institute of Mathematics, Jagiellonian University, Kraków, Poland

(Received September 11, 2003)

This paper is a continuation and development of the dissertation [1]. Complex folded-plate structures with holes are analyzed using the Trefftz-type finite elements, which appears very effective. The shape functions of these elements (Trefftz functions) fulfill respective differential equations. Then, a certain optimization algorithm is proposed, in which an optimized structure can have a large number of parameters used as optimization variables. Therefore, in particular stages of the proposed procedure, less important variables can be eliminated. The choice of the active variable set is based on investigation of sensitivity of the objective function and constraints on small changes of these variables.

Keywords: Trefftz-type finite elements, Hybrid elements, Folded-plate structures, Optimization of structures.

1. Introduction

The paper deals with analysis and optimization of folded-plate structures, however, a large part of the considerations below concerns more general engineering problems. The main purpose of the work is to enhance an optimization algorithm in the case of a wide class of 3D thin-walled structures with openings (Fig. 1). This improvement can follow four directions:

I. Possible minimization of computational time of a single solution inside optimization loops,
II. Modifications of the objective function and constraints,
III. Selection of variables in particular stages of the optimization algorithm,
IV. Enhanced search for minimum of the objective function.

Until now, the authors investigated only the first three areas [2–5], however, the last -iv- direction is just now being explored (in the present paper the standard gradient procedures are applied).

The most effective improvement of the discussed optimization procedure is visible after application of the Trefftz-type finite elements. In Fig. 2 we can see a hybrid element of this type, first proposed in [6]. Inside the element an analytical solution of a differential equation is proposed in the form (example 2D elasticity):

$$\mathbf{u}(\mathbf{x}) = \mathbf{u}^p(\mathbf{x}) + \mathbf{N}(\mathbf{x})\mathbf{c}, \tag{1}$$

where $\mathbf{u}^p$ is a particular solution, $\mathbf{N}$ is a matrix containing the Trefftz functions and $\mathbf{c}$ is a vector of unknown coefficients.

*Partially supported by FNP (Polish Science Foundation).

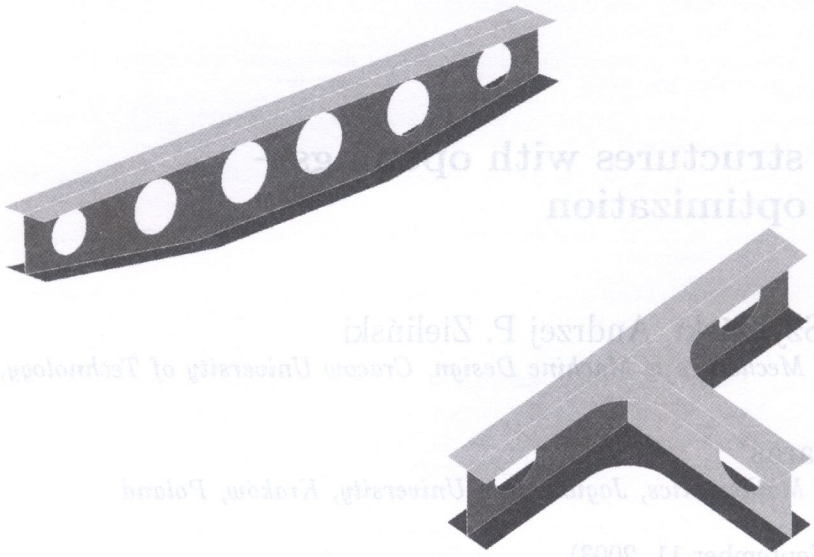

Fig. 1. Examples of 3D plate structures with openings

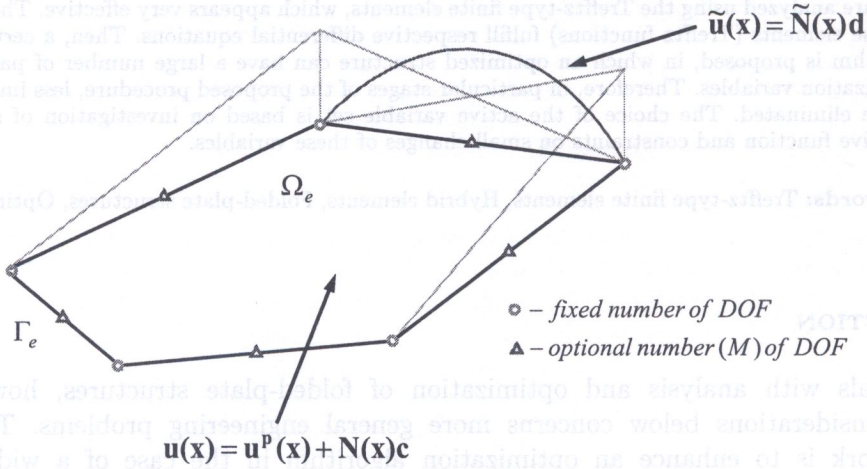

Fig. 2. Hybrid element for plane elasticity

Simultaneously, along the boundary Γ_e a frame function $\tilde{\mathbf{u}}(\mathbf{x})$ is defined (Fig. 2). After analytical calculation of tractions from Eq. (1):

$$\mathbf{t}(\mathbf{x}) = \mathbf{t}^p(\mathbf{x}) + \mathbf{T}(\mathbf{x})\mathbf{c}. \tag{2}$$

The following system of equations can be introduced [7]:

$$\begin{aligned} &\int_{\Gamma_e} \delta\mathbf{t}^{\mathrm{T}}(\mathbf{u} - \tilde{\mathbf{u}})\mathrm{d}\Gamma = 0, \\ &\int_{\Gamma_e} \delta\tilde{\mathbf{u}}^{\mathrm{T}}\mathbf{t}\mathrm{d}\Gamma = \int_{\Gamma_{e_t}} \delta\tilde{\mathbf{u}}^{\mathrm{T}}\bar{\mathbf{t}}\mathrm{d}\Gamma + \delta\mathbf{d}^{\mathrm{T}}\mathbf{r}, \end{aligned} \tag{3}$$

where δ means virtual increment, $\bar{\mathbf{t}}$ are imposed tractions and $\mathbf{r}$ are equivalent nodal forces. Eqs. (3) lead to relation between, $\mathbf{c}$ and $\mathbf{d}$, and finally to the well known finite element form:

$$\mathbf{r} = \mathbf{k}\mathbf{d} + \mathbf{r}^p, \tag{4}$$

where $\mathbf{r}^p$ is a known vector and $\mathbf{k}$ is a symmetric, positive definite stiffness matrix

$$\begin{aligned}
&\mathbf{k} = \mathbf{G}^{\mathrm{T}}\mathbf{H}^{-1}\mathbf{G},\\
&\mathbf{G} = \int_{\Gamma_e} \mathbf{T}^{\mathrm{T}}\tilde{\mathbf{N}}\mathrm{d}\Gamma, \qquad \mathbf{H} = \int_{\Gamma_e} \mathbf{T}^{\mathrm{T}}\mathbf{N}\mathrm{d}\Gamma,\\
&\mathbf{r}^p = \int_{\Gamma_e} \tilde{\mathbf{N}}^{\mathrm{T}}\mathbf{t}^p\mathrm{d}\Gamma - \int_{\Gamma_e} \tilde{\mathbf{N}}^{\mathrm{T}}\bar{\mathbf{t}}\mathrm{d}\Gamma - \mathbf{G}^{\mathrm{T}}\mathbf{H}^{-1}\mathbf{h}, \qquad \mathbf{h} = \int_{\Gamma_e} \mathbf{T}^{\mathrm{T}}\mathbf{u}^p\mathrm{d}\Gamma.
\end{aligned} \tag{5}$$

The above element was investigated in detail in numerous papers, e.g. [7–9], also in the folded-plate version [1, 10]. Its application in optimization procedures is presented in Sec. 3.

2. Folded-plate structures

Spatial structures with large flat panels are widely used in engineering design. These structures can serve as welded girder or box beams supporting big cranes, spans of bridges, folded roofs or flat-walled containers (see Fig. 1). Their common feature is the presence of abrupt change of direction of the outward normal vector while moving along the sides of the non-coplanar panels. In these structures, usually subjected to arbitrary external loads, both bending and membrane effects should be taken into account. Figure 3a presents orientation of a flat panel in 3D space with a local and global coordinate system introduced. In case of the analysis of isotropic linear elastic structures the unknown, modeled displacement field can be expressed as follows:

$$\mathbf{u} = \begin{Bmatrix} u \\ v \\ w \end{Bmatrix} = \sum_{j=1}^{n} \begin{bmatrix} N_{uj}^m & 0 \\ N_{vj}^m & 0 \\ 0 & N_{wj}^b \end{bmatrix} \begin{Bmatrix} c_j^m \\ c_j^b \end{Bmatrix} + \begin{Bmatrix} u^p \\ v^p \\ w^p \end{Bmatrix}. \tag{6}$$

Here, the components $\{u, v\}^{\mathrm{T}}$ correspond to the in-plane displacements (membrane part) and the component $\{w\}$ is the out-of-plane deflection (bending part). The vector $\left\{N_{uj}^m, N_{vj}^m\right\}^{\mathrm{T}}$ contains the T-complete functional set for the membrane part while N_{jw}^b is the j-th T-function for the bending part (the Kirchhoff plate theory is applied). The components $\left\{c_j^m, c_j^b\right\}^{\mathrm{T}}$ are the unknown coefficients and the last vector is the respective particular solution of the analyzed boundary value problem.

A main difficulty, which arises in formulation of the folded plate element, is meeting the conformity conditions between common edges of non-coplanar panels. So far, several concepts for that purpose have been proposed [11, 12]. In case of the T-element formulation (in its p-version) the above problem influences a form of the applied frame function. In the corner nodes only three displacements $\{u, v, w\}^{\mathrm{T}}$ are implemented as nodal degrees of freedom. In the mid-side nodes the number of degrees of freedom is equal to M. This optional number includes parameters describing a constant rotation φ_n, normal to the edge and higher terms both of displacements $\left\{\Delta u^i, \Delta v^i, \Delta w^i\right\}^{\mathrm{T}}$ and normal rotations $\Delta\varphi_n^i$. Such a formulation allows to avoid necessity of introduction of a so-called 'drilling' degree of freedom [11].

The customary force-displacement relationship (4) can be rewritten in a decomposed form as follows (valid for linear, isotropic structures):

$$\mathbf{r} = \begin{Bmatrix} \mathbf{r}^m \\ \mathbf{r}^b \end{Bmatrix} = \begin{bmatrix} \mathbf{k}^m & 0 \\ 0 & \mathbf{k}^b \end{bmatrix} \begin{Bmatrix} \mathbf{d}^m \\ \mathbf{d}^b \end{Bmatrix} + \begin{Bmatrix} \mathbf{r}^{pm} \\ \mathbf{r}^{pb} \end{Bmatrix}. \tag{7}$$

Here, index m corresponds to the membrane part while index b is responsible for the bending part. The above equation is valid for each flat panel, which can be modeled by only one T-element. In

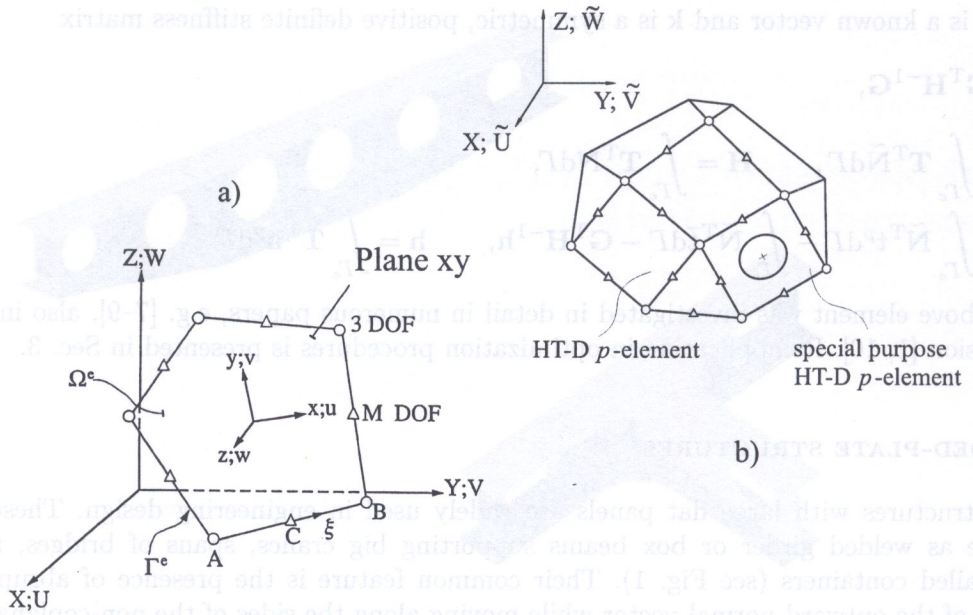

Fig. 3. T-element for folded-plates a) and exemplary mesh for 3D structure with holes b)

case of more complex, spatial structures – Figure 3 – the force-displacement relationship is expressed in a global coordinate system.

The resulting displacements and stresses for each flat panel are obtained analytically with the use of T-functions in any point within each element.

In case of the standard T-elements the system of T-functions consists of polynomials, which are easily generated. A more complex form of T-functions should be applied when we consider special T-elements, from which a T-element with a circular hole inside is a typical example. In this case the set of T-functions can be expressed in polar coordinates (r, θ) and must include terms with both positive and negative exponents of the radius r.

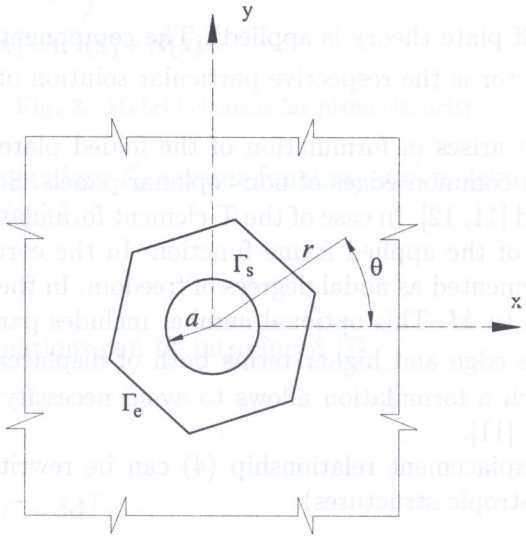

Fig. 4. Part of infinite plate with stress-free circular hole

The formulae shown below present several terms of the T-function set used for the bending state in the case of the stress-free inner boundary Γ_s of the hole (Fig. 4) [7]:

$$N_1 = \ln\rho + \frac{1-\mu}{2(1+\mu)}\rho^2, \tag{8}$$

$$N_2 = \left(\rho^3 - \frac{3+\mu}{1-\mu}\rho^{-1}\right)\cos\theta, \qquad N_3 = \left(\rho^3 - \frac{3+\mu}{1-\mu}\rho^{-1}\right)\sin\theta. \tag{9}$$

The next terms can be generated with the help of the following functions:

$$\begin{aligned} f_k(\rho) &= \frac{1}{k}\frac{3+\mu}{1-\mu}\rho^k + \frac{1}{\rho^{k-2}} - \frac{k-1}{k}\frac{1}{\rho^k}, \\ g_k(\rho) &= \rho^{k+2} - \frac{k+1}{k}\rho^k - \frac{1}{k}\frac{3+\mu}{1-\mu}\frac{1}{\rho^k}, \end{aligned} \tag{10}$$

where μ is the Poisson ratio, ρ is the non-dimensional radius ($\rho = r/a$) and $k = 2, 3, \ldots$ and:

$$\begin{aligned} N_{l+1} &= f_k(\rho)\cos k\theta, \qquad N_{l+2} = g_k(\rho)\sin k\theta, \\ N_{l+3} &= f_k(\rho)\sin k\theta, \qquad N_{l+4} = g_k(\rho)\cos k\theta, \end{aligned} \tag{11}$$

where $l = 4(k-1)$. For simplicity the index denotations – b, m – in Eqs. (8, 9, 11) are omitted.

3. Presentation of optimization algorithm

In structural optimization procedures a basic, gradually modified solution must be repeated very many times inside the optimization loops. In case of complex spatial structures, many various design variables can influence an optimal shape of a structure. It usually results in growth of the optimization space and significantly increases time of calculations in each optimization loop. As it was mentioned before, a considerable decrease of the computational time in comparison to a standard FE solution is observed after application of the Trefftz hybrid element approach.

The benefits of application of the T-elements are presented in the example of 3D-plate structure with holes, which is shown in Fig. 5. For that purpose two comparative studies were performed, first with the T-elements applied, and then with the classical FE ANSYS® solution [13]. In all the present investigations the authors applied a unified objective function - a total volume V of the structure and a stress constraint in the strong form:

$$h = \max_{x\in\Omega}\sigma_0(x) \le h_0\,, \qquad h_0 = 210 \pm 5\ [\mathrm{MPa}], \tag{12}$$

where σ_0 and h_0 are the equivalent and admissible stresses respectively. The tolerance in (12) means that the constraint becomes active when the value of h reaches any point inside the acceptable range. It is worth noting that also other types of objective functions and weak-form constraints were earlier taken into account [4].

The analyzed structure, simply supported at both ends, was subjected to an external constant pressure load imposed symmetrically with respect to the $B - C$ line on the 2nd and 3rd section of panels (see Fig. 6):

- 1st section of panels: $p_{y1} = 0.0$ [N/mm^2],
- 2nd section of panels: $p_{y2} = -0.3$ [N/mm^2],
- 3rd section of panels: $p_{y3} = -0.4$ [N/mm^2].

Due to the symmetry of the applied load and the structure geometry, a set of only six design variables was chosen for optimization:

- radii of holes: $r1$, $r2$, $r3$,
- thickness of ribs: $t1$, $t2$, $t3$.

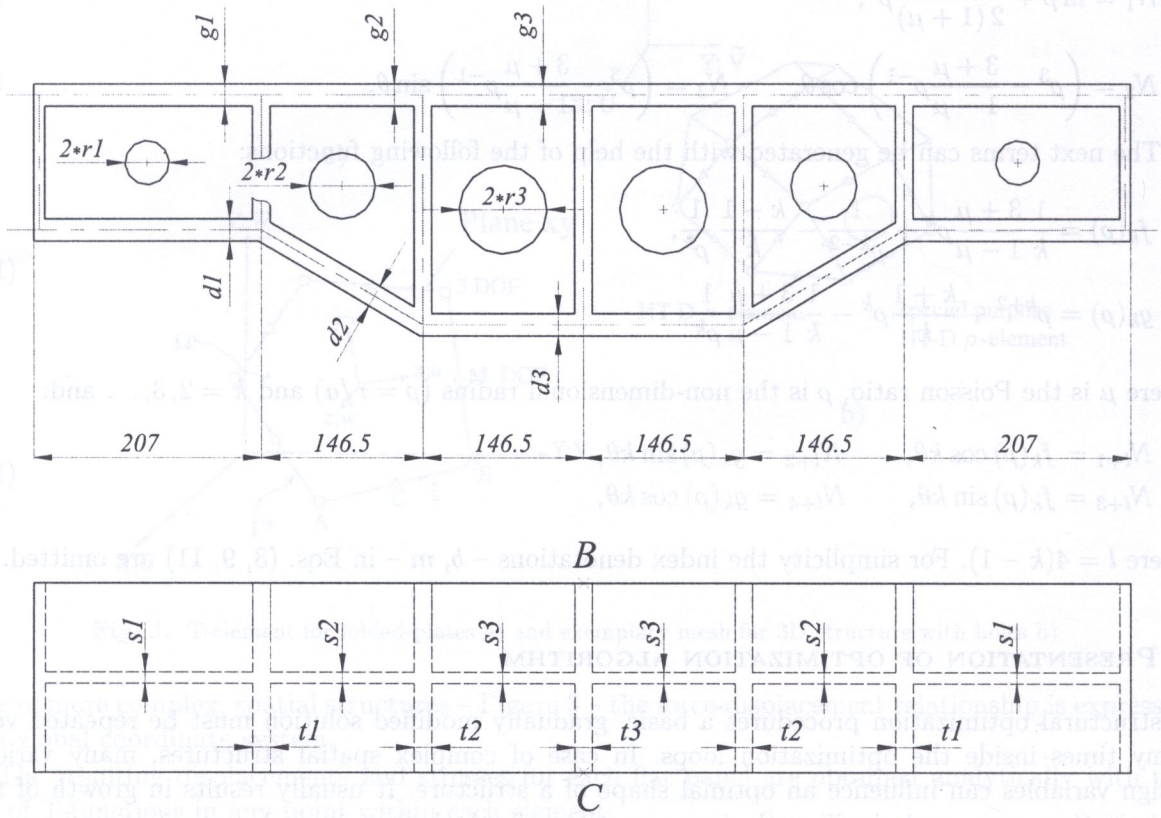

Fig. 5. Optimized simply supported girder

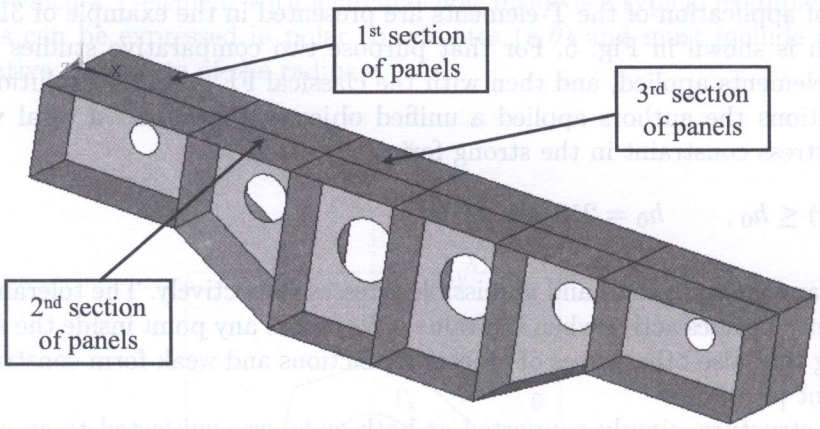

Fig. 6. Mesh of T-elements applied

Admissible values of the design variables were limited by the size of the panels (maximum radii of holes) and by the estimated local buckling conditions (minimum thickness of side ribs):

$$r1 \in \langle 10, 45\rangle\,, \quad r2 \in \langle 20, 62\rangle\,, \quad r3 \in \langle 30, 65\rangle\,, \quad t1, t2, t3 \in \langle 2.0, 6.0\rangle\,. \tag{13}$$

Additionally, the step-wise change of the design variables was assumed, with the step equal to 1 [mm] for the hole radius and 0.5 [mm] for the rib thickness. In case of the T-element approximation the whole structure was modeled with the use of only 44 large elements (Fig. 6). This resulted in a relatively small number of nodal active degrees of freedom – $N_{\mathrm{ACT}} = 1571$ (maximum polynomial

degree $k = 11$). In case of application of the standard FEM, the number of applied elements was many times higher. This was caused mainly by presence of the holes in the central panels. Because of these strong stress concentrators, the finite element mesh had to be locally refined around the holes. To obtain results acceptable from the engineering point of view (Zienkiewicz – Zhu error estimator lower than 5%), the mesh with $N_{\mathrm{ACT}} \cong 140000$ had to be applied.

In case of the folded-plate structures the maximum stress may appear both on the top or bottom sides of panels. Hence the number of points, in which the value of equivalent stress should be controlled is almost doubled in comparison with the number of nodal points applied in the mesh (only certain narrow zones located along the lines of folds are excluded from this analysis). This drastically increased the calculation time for each optimization loop and the total time of optimization. For ANSYS® calculations [13] it was equal to ca. 10 [hours], while in case of T-elements it was only 1 [hour].

The rough scheme of optimization algorithm is presented in Fig. 7. The size of holes in the central panels for the starting structure was assumed on the base of engineering formulae suggested for calculations of structures with holes [14]. In the above scheme the applied stop condition needs a certain comment. It acted and finished the procedure in two cases:

- when in several consecutive steps (optimization loops) decrease of the objective function was negligible or of sufficiently small oscillating form,
- when the design variables approached their upper or lower limits.

In the analyzed girder mainly the latter form of the stop condition was active.

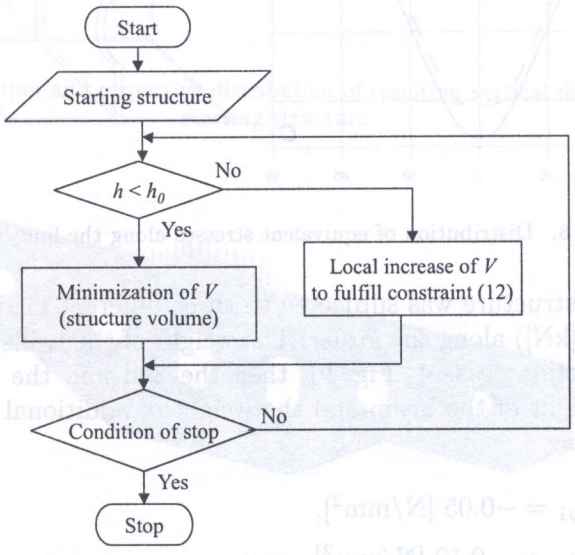

Fig. 7. Scheme of optimization algorithm

Table 1 presents the comparison of results which were obtained for the classical FE and Trefftz-type calculations. As it can be seen, both results for the starting and final structure remain in satisfactory agreement. Additionally, the zones of maximum stress are located at the same areas for the starting and final structures in both types of calculations. The observed reduction of total volume approaches 16%.

Figure 8 presents comparison of distributions of equivalent stresses along the line $B - C$ obtained in the optimal structure for calculations made with the classical FE ($N_{\mathrm{ACT}} \cong 140000$) and T-elements ($N_{\mathrm{ACT}} = 1571$) respectively. Again, the presented results are in good agreement along the whole line.

The next numerical study also concerned the structure presented in Fig. 5. The starting values for radii of holes and thickness of panels were assumed the same as in the above presented analysis.

Table 1

Values of design variables	Maximum stress σ_{eqv}^{max} [MPa]	
	Classical FE	T-elements
Starting structure: r1/r2/r3 = 20./30./40. t1/t2/t3 = 4.0/4.0/4.0	211.27*	208.06*
Optimal structure: r1/r2/r3 = 26./61./65. t1/t2/t3 = 2.0/2.0/2.0	214.98**	210.96**

* – maximum localized on the top panel,

** – maximum localized on boundary of hole with radius $r1$.

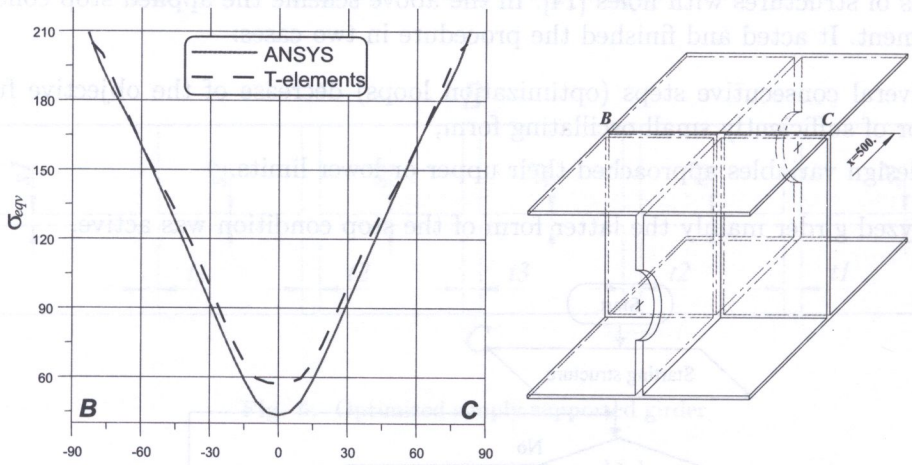

Fig. 8. Distribution of equivalent stresses along the line $B - C$

In this case, however, the structure was subjected to three different load systems, which simulated movement of a trolley (10 [kN]) along the girder. The weight of the trolley was applied to the whole upper panel of the 1st section (case 1, Fig. 9), then the 2nd and the 3rd one (case 3, Fig. 10). The approximate dead weight of the beam and the weight of additional equipment was taken into account in the following way:

- 1st section of panels: $p_{y1} = -0.05$ [N/mm^2],
- 2nd section of panels: $p_{y2} = -0.10$ [N/mm^2],
- 3rd section of panels: $p_{y3} = -0.15$ [N/mm^2].

The distribution of resulting vertical displacements for cases 1 and 3 are shown in Figs. 9 and 10.

The following set of variables was now chosen for optimization (see Fig. 5):

- radii of holes $r1$, $r2$, $r3$,
- thickness of ribs $t1$, $t2$, $t3$,
- thickness of top section panels $g1$, $g2$, $g3$,
- thickness of bottom section panels $d1$, $d2$, $d3$,
- thickness of panels with holes $s1$, $s2$, $s3$.

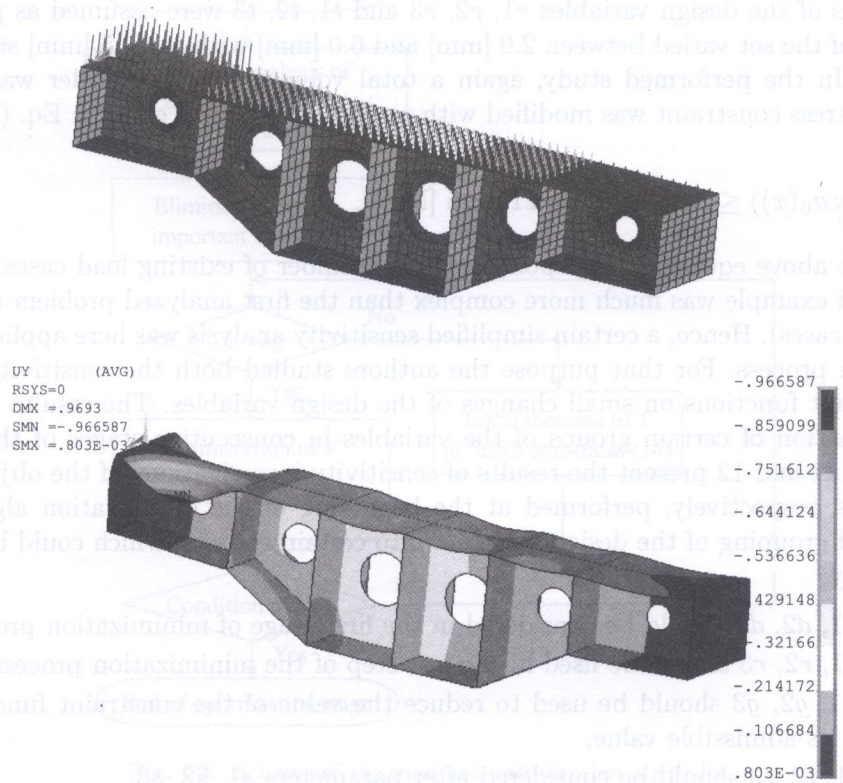

Fig. 9. Load case 1 illustration and respective distribution of resulting vertical displacements (in [mm]) for starting structure

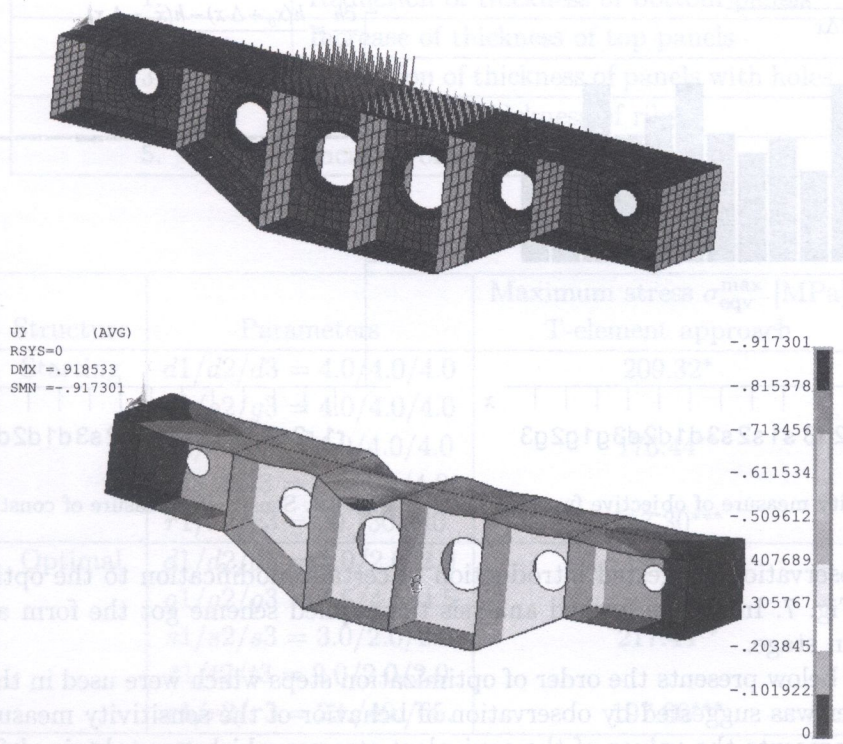

Fig. 10. Load case 3 illustration and respective distribution of resulting vertical displacements (in [mm]) for starting structure

The symmetry of the structure was also taken into account. The step-wise change and the admissible values of the design variables $r1$, $r2$, $r3$ and $t1$, $t2$, $t3$ were assumed as previously. The remaining part of the set varied between 2.0 [mm] and 6.0 [mm] with the 0.5 [mm] step-wise change of their values. In the performed study, again a total volume V of the girder was the objective function and a stress constraint was modified with respect to the form given in Eq. (12) (h_0 slightly higher):

$$h = \max_i(\max_{x\in\Omega}\sigma_0(x)) \leq h_0\,, \qquad h_0 = 215 \pm 5\ [\text{MPa}]. \tag{14}$$

Index i in the above equation corresponded to the number of existing load cases.

The discussed example was much more complex than the first analyzed problem (15 design variables and 3 load cases). Hence, a certain simplified sensitivity analysis was here applied to accelerate the optimization process. For that purpose the authors studied both the sensitivity of the objective and constraint functions on small changes of the design variables. The results of this analysis suggested elimination of certain groups of the variables in consecutive stages of the optimization process. Figures 11 and 12 present the results of sensitivity investigations of the objective and constraint functions, respectively, performed at the beginning of the optimization algorithm. These results suggested grouping of the design variables into certain subsets, which could be concluded in the following way:

- parameters $d1$, $d2$, $d3$ should be considered in the first stage of minimization procedure,
- parameters $r1$, $r2$, $r3$ should be used in the last step of the minimization process,
- parameters $g1$, $g2$, $g3$ should be used to reduce the value of the constraint function in case of crossing over its admissible value,
- parameters $t1$, $t2$, $t3$ should be considered after parameters $s1$, $s2$, $s3$.

The first two conclusions were justified by results of the sensitivity of the objective function and the last two by the sensitivity of the constraint function.

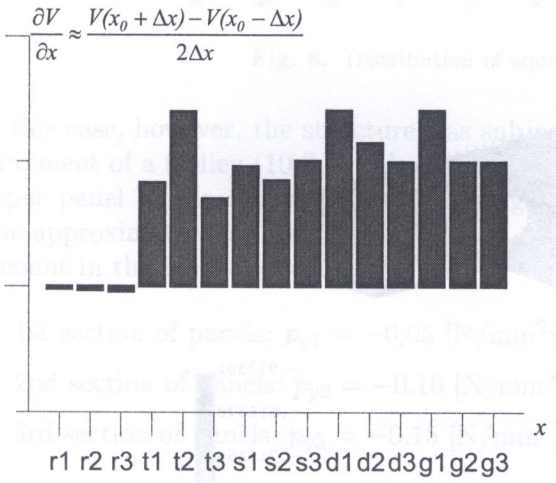

Fig. 11. Sensitivity measure of objective function V

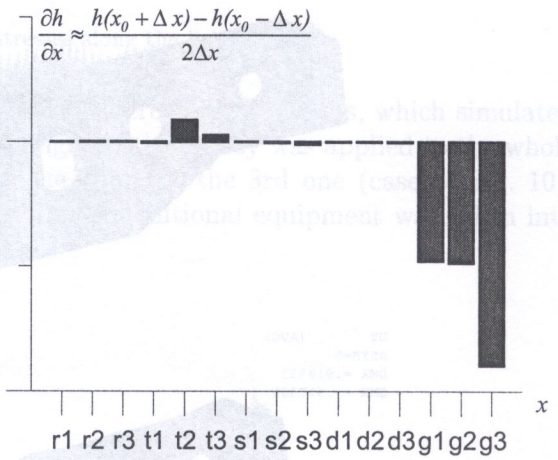

Fig. 12. Sensitivity measure of constraint function h

The above observation suggested introduction of certain modification to the optimization algorithm given in Fig. 7. In the performed analysis the applied scheme got the form as in Fig. 13 in each optimization stage.

Table 2 given below presents the order of optimization steps which were used in the optimization stages. This order was suggested by observation of behavior of the sensitivity measures.

The Table 3 presents the values of the equivalent stresses which were obtained for the starting and final structure. These results were obtained with the T-element approach. The reduction of the total volume reached now 31% .

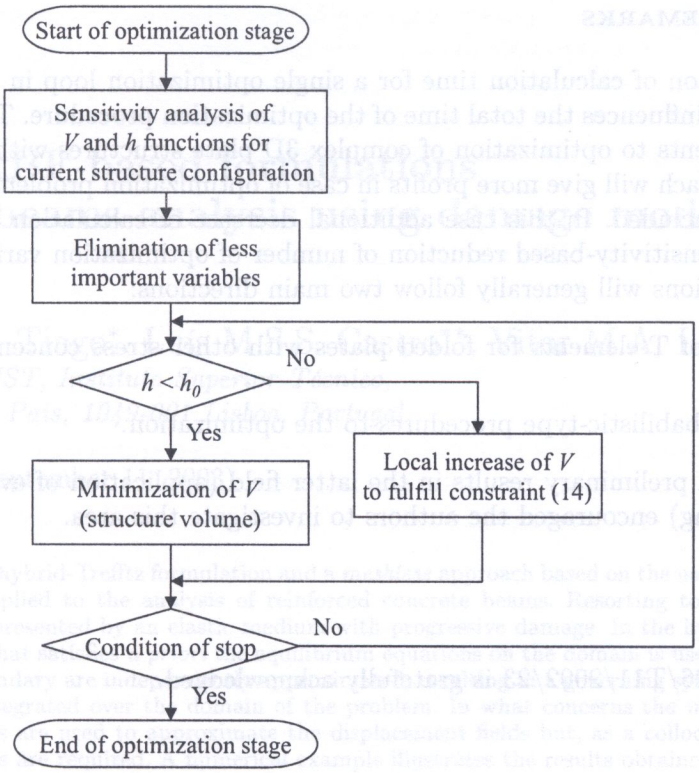

Fig. 13. Scheme of the modified optimization algorithm

Table 2

No. of optimiz. step	
1.	Reduction of thickness of bottom panels
2.	Increase of thickness of top panels
3.	Reduction of thickness of panels with holes
4.	Reduction of thickness of ribs
5.	Increase of diameters of holes

Table 3

Structure	Parameters	Maximum stress $\sigma_{\text{eqv}}^{\max}$ [MPa] T-element approach
Starting	$d1/d2/d3 = 4.0/4.0/4.0$	209.32*
	$g1/g2/g3 = 4.0/4.0/4.0$	
	$s1/s2/s3 = 4.0/4.0/4.0$	176.44**
	$t1/t2/t3 = 4.0/4.0/4.0$	
	$r1/r2/r3 = 20./30./40.$	217.30***
Optimal	$d1/d2/d3 = 2.0/2.0/2.0$	190.59*
	$g1/g2/g3 = 4.5/4.5/4.5$	
	$s1/s2/s3 = 3.0/2.0/2.0$	217.44**
	$t1/t2/t3 = 2.0/2.0/2.0$	
	$r1/r2/r3 = 23./49./65.$	197.66***

* – results for 1st load case,
** – results for 2nd load case,
*** – results for 3rd load case.

4. Concluding remarks

The observed reduction of calculation time for a single optimization loop in case of the T-element approach drastically influences the total time of the optimization procedure. This justifies the application of the T-elements to optimization of complex 3D plate structures with stress concentrators. The T-element approach will give more profits in case of optimization problems with higher number of design variables included. In this case additional decrease of calculation time can be observed when applying the sensitivity-based reduction of number of optimization variables [2, 4].

Further investigations will generally follow two main directions:

- the development of T-elements for folded plates with other stress concentrators, e.g. V- or U-notches;
- application of probabilistic-type procedures to the optimization.

Especially, certain preliminary results in the latter field (application of evolutionary algorithms or simulated annealing) encouraged the authors to investigate this area.

Acknowledgment

Grant KBN PB - 0826/T11/2002/23 is gratefully acknowledged.

References

[1] B. Szybiński. *Trefftz-type finite elements applied to the analysis of complex thin-walled structures.* PhD thesis, Cracow University of Technology, 1997.

[2] H. Sanecki, A.P. Zieliński. Trefftz finite element approach: acceleration of optimization process by sensitivity analysis. In: *Proc. of the 1st ECCM*, Munich, Germany, 1999.

[3] M. Karaś. Generalized Trefftz method applied to optimization of elastic structures. *PhD thesis*, Cracow University of Technology, 2001.

[4] A.P. Zieliński, H. Sanecki, M. Karaś. Effectiveness of the Trefftz method in different engineering optimization procedures. *CAMES*, **8**: 479–493, 2001.

[5] B. Szybiński, M. Karaś, A.P. Zieliński. 3D plate structures: optimization using special T-elements. In: *Proc. of the V World Congress on Computational Mechanics*, Vienna, Austria, 2002.

[6] J. Jirousek. Basis for development of large finite elements locally satisfying all field equations. *Comp. Meth. Appl. Mech. Engng*, **14**: 65–92, 1978.

[7] J. Jirousek, L. Guex. The hybrid-Trefftz finite element model and its application to plate bending. *Int. Journal for Num. Meth. in Engng*, **23:** 651–693, 1986.

[8] J. Jirousek, A. Venkatesh. Hybrid-Trefftz plane elasticity elements with p-method capabilities. *Int. Journal for Num. Meth. in Engng*, **35**: 1443–1472, 1992.

[9] J. Jirousek, A.P. Zieliński. Survey of Trefftz-type element formulations. *Computer & Structures*, **63**(2): 225–242, 1997.

[10] J. Jirousek, B. Szybiński, A.P. Zieliński. Study of a family of hybrid Trefftz folded plate p-version elements. *CAMES*, **4**(3–4): 453–476, 1997.

[11] T.J.R. Hughes, F. Brezzi. On drilling degrees of freedom. *Comp. Meth. Appl. Mech. Engng*, **72**: 105–121, 1989.

[12] O.C. Zienkiewicz, R.L. Taylor. The Finite Element Method. *Butterworth–Heinemann*, 5th edition, 2000.

[13] Analysis System Inc., Swanson. *ANSYS – User Manual*, 1999. Release 5.7.

[14] R. Bares. Tables for the Analysis of Plates, Slabs and Diaphragms Based on the Elastic Theory. *Bau Verlag Gmbh*, Wiesbaden, 1990.